Int J Clin Exp Pathol 2018;11(2):1009-1017
www.ijcep.com /ISSN:1936-2625/IJCEP0071460

Original Article

Centella asiatica inhibits renal interstitial fibrosis by regulating Smad3 and Smad7 expression in the TGFβ signaling pathway

Zhu Zhang[1,2], Jiwei Ma[1], Rui Feng[1], Zheng Wang[1]

[1]*Department of Nephrology, The First Affiliated Hospital of Henan Traditional Chinese Medical University, Zhengzhou, China;* [2]*Department of Nephrology, Fuwai Central China Cardiovascular Hospital, Zhengzhou 450000, China*

Received December 24, 2017; Accepted January 17, 2018; Epub February 1, 2018; Published February 15, 2018

Abstract: *Centella asiatica* (CA) is a well-known traditional Chinese herb with a long history of therapeutic uses. In the present study, we evaluated the effect of CA granula on renal interstitial fibrosis, as well as Smad3 and Smad7 in a TGF-β signaling pathway mediated mechanism. Fifty adult SD male rats were randomly divided into five groups: sham-operated; unilateral ureteral obstruction (UUO); Monopril; high-dose CA (CA (H)); and low-dose CA (CA (L)). Blood samples were collected 14 days after oral gavage and the blood urea nitrogen (BUN) and serum creatinine (Scr) was measured. H&E and Masson straining were utilized to determine the renal tubule interstitial fibrosis. Smad3 and Smad7 mRNA and protein levels were determined in kidney tissues by immunohistochemistry, real-time PCR, and Western blot analysis respectively. Compared with the UUO group, the CA treatment significantly inhibited renal interstitial fibrosis and Smad3 expression, but increased Smad7 expression at both mRNA and protein levels in a dose-dependent manner. Our research suggests that CA administration could delay renal interstitial fibrosis by inhibiting Smad3 but promoting Smad7 expression in TGF-β pathways, without obvious liver or kidney toxicity.

Keywords: Centella asiatica granula, renal interstitial fibrosis, TGF-β, Smad3, Smad7

Introduction

In recent years, the prevalence of chronic kidney disease (CKD) has significantly increased. Its characteristics of occult onset may easily cause a patient to miss the best period for checking the progress of the disease, which may lead to progression to end-stage renal disease (ESRD), resulting irreversible kidney failure. The latest epidemiological survey data (2012) showed that the CKD prevalence rate among China's adult population was 10.8%. However, the awareness rate was only found to be 12.5% [1], which resulted in heavy economic and psychological burdens to the patients and their families. Therefore, chronic kidney disease has currently become an important public health problem in China. It is particularly urgent and necessary to explore the mechanism of this disease, and to investigate effective new drugs for the prevention and treatment of CDK.

The renal damage due to the pathological factors, such as injury, inflammation, obstruction, etc. will induce extracellular matrix (ECM) pathological deposition in the kidneys, leading to an over-proliferation of the positive myofibroblast of the α-smooth muscle actin (α-SMA), and finally cause renal tubule interstitial fibrosis (TIF) [2]. The disruption of renal structures caused by TIF is a common cause of the progression of various types of renal disease [3, 4]. Therefore, inhibiting the occurrence and development of TIF is an effective method by which to retard progression of CKD to ESRD. It is known that, during progression of TIF, its characteristic pathological change is Epithelial-Mesenchymal Transition (EMT). Transforming growth factor β1 (TGF-β1) is the key factor which promotes renal fibrosis, and an activated TGF-β signaling system will mediate the occurrence and progression of EMT [5]. The smooth muscle actin (Smad) system, as the TGF-β intracellular signaling molecule, could regulate cell membrane signal transduction by activated Smad proteins (Smad2 and Smad3) and the inhibitory Smad protein (Smad7) [6].

The chemical composition of *Centella asiatica (L) Urban* includes triterpenoid acid, triterpenoid saponin, polyyne alkene, volatile oil, etc [7]. Previous studies have shown that asiaticoside could inhibit over-proliferation of fibroblasts, and decrease the acid puffball polysaccharide and collagen, as well as reduce collagen synthesis by inhibiting the activities of the transpeptidase. Asiaticoside may further effectively control the overgrowth of the stroma and fibrous components of the connective tissue, and treat the scleroderma by inhibiting hyperplasia of the unordered fibrous connective tissue. It has been shown that the effects of asiaticoside are related to the Smad signal pathway [8, 9]. It was also proven that the mechanism of asiaticoside's inhibition of collagen hyperplasia was mainly to inhibit the pathologic action of TGF-β1 by increasing expression of Smad7, thereby effectively inhibiting fibroblast proliferation [10].

This study established a unilateral ureteral obstruction (UUO) rat model, and evaluated the impact of CA on the expressions of Smad3 and Smad7 in the TGF-β pathway in rat kidney tissue. The Fosinopril Sodium Tablets (Monopril) served as the control group for its obvious inhibiting effects on renal fibrosis. This study further aimed to provide experimental evidence on the targets of CA for the treatment of the renal tubule interstitial fibrosis.

Materials and methods

Animal model

In this study, all of the animal procedures were conducted in accordance with the *Guidelines for Care and Use of Laboratory Animals*, and were approved by the Animal Care and Use Committee at the First Affiliated Hospital, Henan University of Traditional Chinese Medicine. A total of 50 male adult Sprague-Dawley (SD) rats, with weights of 200 (±20) g, were supplied by the Vital River Laboratories, Beijing, China. The rats were randomly divided into five groups as follows: the sham-operated group; model group; fosinopril group; high-dose Centella asiatica group (CA (H)); and low-dose Centella asiatica group (CA (L)). There were 10 rats allocated to each group. Rats from the surgery group were anesthetized by intraperitoneal injection using 10% chloral hydrate (0.3 ml/100 g) solution. In the model group, UUO surgery was performed under general anesthesia. An incision was made on the left abdomen to expose the left kidney and ureter, which was subsequently ligated and cut from the proximal inferior pole of the left kidney. The sham-operated group had their ureters exposed and manipulated without ligation. The intragastric administration was implemented at a fixed time each day for 14 days, and the dosages of CA granula were 5.6 mg/100 g/day, and 16.8 mg/100 g/day for CA (L) and CA (H) group. The dosages of the fosinopril group (Monopril group) were 1.67 mg/100 g/day, and equivalent saline solutions were administered to the sham-operated and model groups.

Biochemical index and histopathological examination

At 14 days after the intragastric administration, 4 ml blood samples were obtained from abdominal aorta, and rate urea nitrogen and rat creatinine test kits (Jingkang Biological Engineering, Shanghai, China) were used to detect the serum urea nitrogen (BUN), and serum creatinine (Scr). Meanwhile, the left kidneys were removed, and paraffin embedding was performed after fixing with 4% paraformaldehyde. The tissue sections were gradient dehydrated using ethyl alcohol, made transparent with xylene, and immersed in paraffin for 3 h at 62°C. A 4 μm paraffin section was then used for the H&E and Masson staining. Slides were examined and pictures taken using a microscopic image acquisition system (BX 41).

Immunohistochemical analysis

The paraffin-embedded renal tissue section was cut into 4 μm slides, deparaffinized and rehydrated. The slides were incubated with primary antibodies of the rabbit anti-rat Smad3 and Smad7 (1:100; Bioss, Beijing, China) overnight at 4°C. The biotinylated goat anti-rabbit IgG were added for 20 minutes at 37°C. Finally, the DAB-H2O2 (Boster Biological Engineering Co. Ltd., Wuhan, Hubei, China) developing was performed, hematoxylin staining was applied for counterstaining, and the slides were covered for microscopic examination. Ten views of renal tubular interstitial from each slide were then randomly recorded under high magnification (×400), and Image Pro Plus 6.0 analysis software was used for the analysis. The yellow or brown granules in the cytoplasm were recorded as the positive signal. The average optical density (OD) of the positive staining and

Table 1. Primers for quantitative PCR analysis

Name	Sequence	Product size (bp)
Smad3	F: 5'-AGACACCAGTGCTACCTCCA-3' R: 5'-CCAGCGGGGAAGTTAGTGTT-3'	363
Smad7	F: 5'-GGAGTCCTTTCCTCTCTC-3' R: 5'-GGCTCAATGAGCATGCTCAC-3'	130
β-actin	F: 5'-CCCATCTATGAGGGTTACGC-3' R: 5'-TTTAATGTCACGCACGATTTC-3'	450

Table 2. Comparison of biochemical indices of the rats in each group (mean ± SD)

Groups	n	BUN (mmol/L)	SCR (μmol/L)
Sham	10	5.4400±0.66885	20.0100±0.28102
UUO	8	8.7130±0.92259*	28.3400±0.67278*
Monopril	10	8.4250±0.24042#	31.4000±0.24185#
CA (H)	9	7.6490±0.17390#	30.6100±0.35570#
CA (L)	10	8.4490±0.18574#	26.8600±0.10723#

*P<0.05, compared with the sham group; #P>0.05, compared with the model group.

background after chroma transformation were calculated.

Fluorescent quantitative PCR

The total RNA of the rats' renal tissue was extracted using TRIzol (Life Technologies, Carlsbad, CA, USA) according to the manufacturer's instructions. The total RNA from each group was then reverse transcribed to cDNA using a RevertAid first strand cDNA synthesis kit (K1622; Thermo Fisher Scientific, Waltham, MA, USA). PCR was performed using an SYBR Green PCR Kit (Invitrogen Life Technologies, USA) in an ABI 7300 Real-Time PCR System (Applied Biosystems, Foster City, CA, USA). The primers for quantitative PCR analysis are detailed in **Table 1**. The PCR reaction was 50°C for two minutes; 95°C for 10 minutes; 95°C for 15 seconds; 60°C for one minute, for a total of 40 cycles; 95°C for 15 seconds; and 60°C for 15 seconds. The fluorescence signal was collected in the annealing stage. The fluorescent quantitative PCR results were expressed by the Ct value, and a relative quantitative method ($2^{-\Delta\Delta Ct}$) was adopted.

Western blot

The supernatant from the renal tissues was taken after homogenation, and a BCA Protein Assay Kit (Solarbio Science and Technology Co., Ltd., Beijing, China) was used to test the protein concentration. Equivalent tissue protein samples were taken and transferred to the PVDF membrane (Pierce Biotechnology, Rockford, IL, USA) after 10% SDS-PAGE separation. TBST containing 5% skim milk powder was used to block for one hour under room temperature. The samples were then incubated overnight with the specific Smad3 (1:2000) antibody and Smad7 antibody (1:3000; Abcam, Cambridge, MA, USA), respectively. After the membranes were washed, they were allowed to interact for one hour with the second antibody coupling with horse radish peroxidase (ZSGB-BIO, Beijing, China) under room temperature. Following sufficient washing, ECL chemiluminescent liquid A and B were then added onto the membrane according to a ratio of 1:1. A Universal Gel Document System (Image Lab) was used to obtain the images, and to analyze the optical density of the target bands.

Statistical analysis

In this study, data are presented as mean ± SD. Statistical significance tests were performed using SPSS software version 18.0. The comparison between groups was examined using a one-way analysis of the variance (ANOVA). $P<0.05$ was taken as a statistically significant difference.

Results

CA had no impact on the biochemical index of the rat in the UUO model

The results are detailed in **Table 2**. When compared with the sham-operated group, the BUN and SCR values of the rats in the UUO model group had obviously increased ($P<0.05$), and there were no obvious changes after the CA treatment ($P>0.05$).

CA improved renal morphology in the UUO rats

The results are shown in **Figure 1**. There were no histopathological changes in the kidney in the sham group. In the UUO model group, the renal tubule lumen expansion and the tubule walls stiffness and deformation was observed, accompanied by the tubular basement membranes atrophy, deformations and partial loss. There was obvious inflammatory cell infiltration

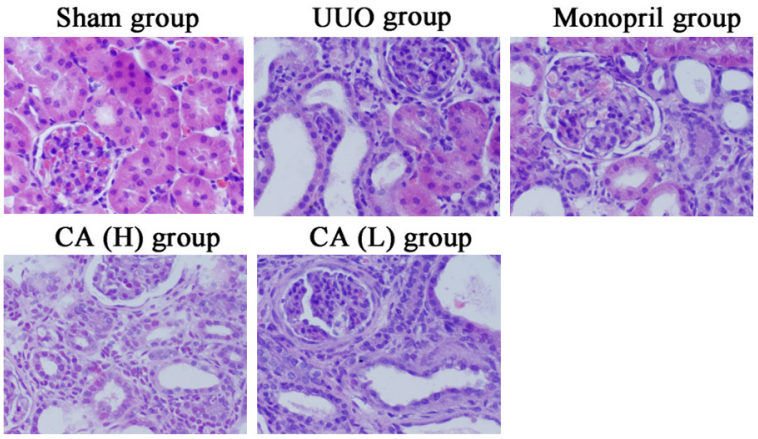

Figure 1. Treatment of CA improved renal morphology in the UUO rats. CA or vehicle control was orally administered in sham- or UUO-operated rats starting on the day of the surgery for 14 days. Representative photomicrographs showed the HE staining of each group.

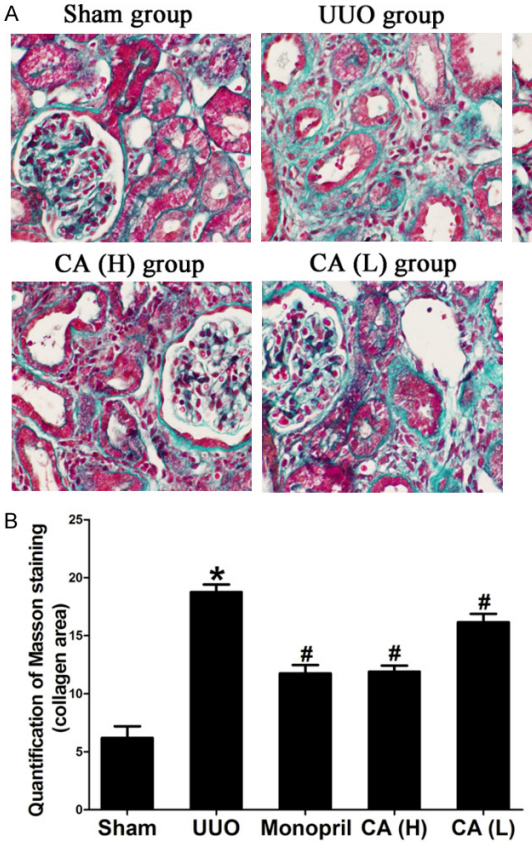

Figure 2. Treatment of CA ameliorated renal fibrosis in the UUO rats. CA or vehicle control was orally administered in sham- or UUO-operated rats starting on the day of the surgery for 14 days. A. Representative photomicrographs show the Masson trichrome staining of each group (400×). B. Quantification of fibrotic area in Masson trichrome–stained kidneys. Error bars represent mean ± SD. *P<0.05 compared with sham group; #P<0.05 compared with UUO group.

in the renal interstitium. Furthermore, the renal interstitium was enlarged, and the extracellular matrix was accumulated. CA treatment significantly improved the renal morphology in the UUO rats.

CA inhibited the renal fibrosis of the UUO rats

The results are shown in **Figure 2**. The green collagen of the sham operated group was found to be mainly distributed on the basal membrane of the renal capsule, tubular basement membrane, mesangial area, and Bowman's capsule wall, with less interstitial expression observed. The green collagen of the UUO group was mainly distributed in the abovementioned areas, and the renal interstitial was obviously widened. Also, the green area in the interstitial was significantly increased, indicating that mass collagenous fibers had accumulated in the renal interstitial area, and the degree of fibrosis was obviously higher than that of the sham operated group ($P<0.05$). The green area of CA treatment group was found to be obviously decreased when compared with the model group ($P<0.05$), which indicated that both the CA and Monopril could inhibit the renal tubule interstitial fibrosis. Among these, the CA (H) group, as well as the Monopril group, had equivalent degrees of collagen expression (P>0.05).

Impact of CA on the Smad3 and Smad7 expressions in renal tissues in the UUO rats

The results are shown in **Figure 3**. The renal tissues in the sham operated group were found to have less Sm-

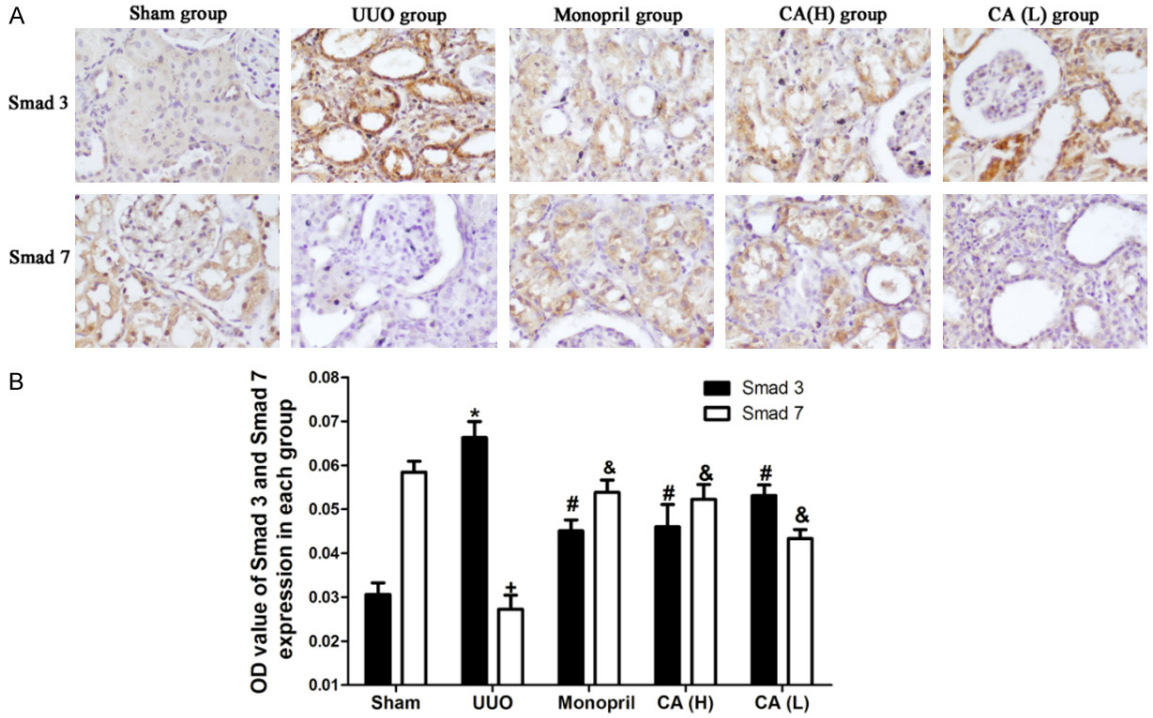

Figure 3. Treatment of CA inhibited Smad3 expression and increased Smad7 expression in the renal tissues of the UUO rats. CA or vehicle control was orally administered in sham- or UUO-operated rats starting on the day of the surgery for 14 days. A. Representative photomicrographs show the immuno-histochemical results of each group (400×). B. Quantification of Smad3 and Smad7 expression in each group. Error bars represent mean ± SD. *P<0.05 compared with Smad3 in sham group; #P<0.05 compared with Smad3 in UUO group; +P<0.05 compared with Smad7 in sham group; &P<0.05 compared with Smad7 in UUO group.

Table 3. Smad3 mRNA and protein expression in each group (mean ± SD)

Groups	n	Smad3 mRNA	Smad3 protein
Sham	10	1.000000±0.0000000	1.000000±0.0000000
UUO	8	2.789377±0.0613903*	1.914895±0.0321774*
Monopril	10	1.533349±0.0444970#	1.254602±0.0403550#
CA (H)	9	1.592549±0.0335374#	1.333943±0.0123628#
CA (L)	10	2.051284±0.0628026#	1.682663±0.0285100#

*P<0.05, compared with the sham group; #P<0.05, compared with the model group.

ad3 expression, with only a small amount of brown positive staining in the kidney tubule and renal corpuscle. The Smad3 expression of the model group was obviously increased, and the renal corpuscle and epithelial cell of the kidney tubule of the rats showed obvious brown expression. Compared with the model group, Smad3 expression in the CA treatment group was significantly decreased (P<0.05). The expression of Smad3 in the CA (H) group was found to be decreased compared with that in the CA (L) group (P<0.05). There was no statistical significance between the CA (H) group and the Monopril control group (P>0.05).

Smad7 in the sham-operated group was mainly expressed in the renal corpuscle and epithelial cell of the kidney tubules and in the model group Smad7 was observed to be significantly decreased. Compared with the model group, the CA treatment group obviously increased the Smad7 expression (P<0.05), and expression of Smad7 in the CA (H) group was higher compared with that of the CA (L) group (P< 0.05). The Monopril and CA (H) groups displayed equivalent expression (P>0.05).

CA inhibited Smad3 gene and protein expression in rats with the UUO model

As shown in **Table 3** and **Figure 4**, compared with the model group, the CA treatment decreased the Smad3 expressions in both the mRNA and protein level in the UUO rat's kidney tissues (P<0.05). The expression of Smad3 in

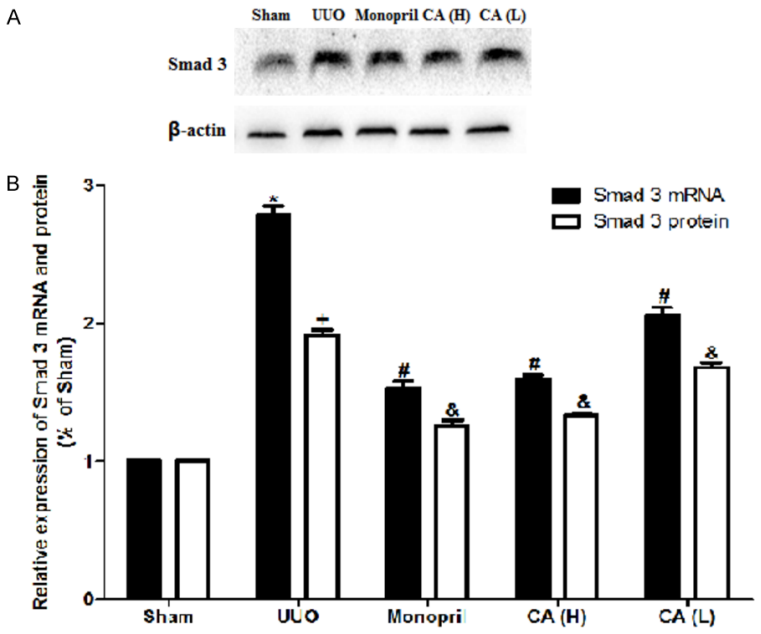

Figure 4. Treatment of CA inhibited Smad3 gene and protein expression in the renal tissues of the UUO rats. CA or vehicle control was orally administered in sham- or UUO-operated rats starting on the day of the surgery for 14 days. A. Smad3 was measured by the Western Blot; B. Quantitative data of the Smad3 mRNA and protein expression analyzed for each group. The error bars represent mean ± SD. *P<0.05 compared with Smad3 mRNA level in sham group; #P<0.05 compared with Smad3 mRNA level in UUO group; +P<0.05 compared with Smad3 protein level in sham group; &P<0.05 compared with Smad3 protein level in UUO group.

Table 4. Smad7 mRNA and protein expression in each group (mean ± SD)

Groups	n	Smad7 mRNA	Smad7 protein
Sham	10	1.000000±0.0000000	1.000000±0.0000000
UUO	8	0.477183±0.0369971*	0.522132±0.0273262*
Monopril	10	0.759414±0.0333397#	1.207967±0.0389462#
CA (H)	9	0.924940±0.0160862#	1.135367±0.0729589#
CA (L)	10	0.656079±0.0361356#	0.812367±0.0078679#

*P<0.05, compared with the sham group; #P<0.05, compared with the model group.

the CA (H) group was found to be decreased compared with the CA (L) (P<0.05), which indicated a dose dependence effect of CA treatment. There were no significant differences observed between the CA (H) group and the Monopril group (P>0.05).

CA increased Smad7 gene and protein expression of the rats in the UUO model

As shown in **Table 4** and **Figure 5**, when compared with the model group, the CA treatment was found to promote the expression of the Smad7 mRNA and protein in the kidney tissues of the UUO rats (P<0.05). Expression in the CA (H) was found to be increased compared with that of the CA (L) group (P<0.05), indicating that the CA treatment could regulate the Smad7 expression in a dose dependent manner.

Discussion

The characteristic manifestations of renal tubule interstitial fibrosis (RIF) include: tubular basement membrane components and interstitial ECM accumulation and the mass propagation of the α-SMA positive myofibroblast. Myofibroblasts are generated by EMT from renal tubular epithelial cells, which leads to massive generation and accumulation of ECM in the interstitial region, and the occurrence of interstitial fibrosis lesions.

EMT is a very complex process of transformation, and is divided into three subtypes [11-14]: type 1, the complex organs and tissues were developed during the gastrula period of the metazoan embryonic development, which was repeatedly involves the EMT and MET processes; type 2, the endothelium or the second epithelium is transformed into tissue fibroblasts, and participates in the wound repair and fibrosis under tissue injuries and inflammation stimulations; and type 3, cancer cells from the epithelium lose polarity, which are transformed into cancer cells with EMT ability.

In 1995, Strutz et al. showed for the first time that EMT was involved in the formation of renal fibrosis [15]. Rastaldi et al. found that there were different degrees of EMT in all of the pathological types, and the number of renal tubular epithelial cells with EMT characteristics was found to be closely related to the serum creatinine concentration and the degree of renal

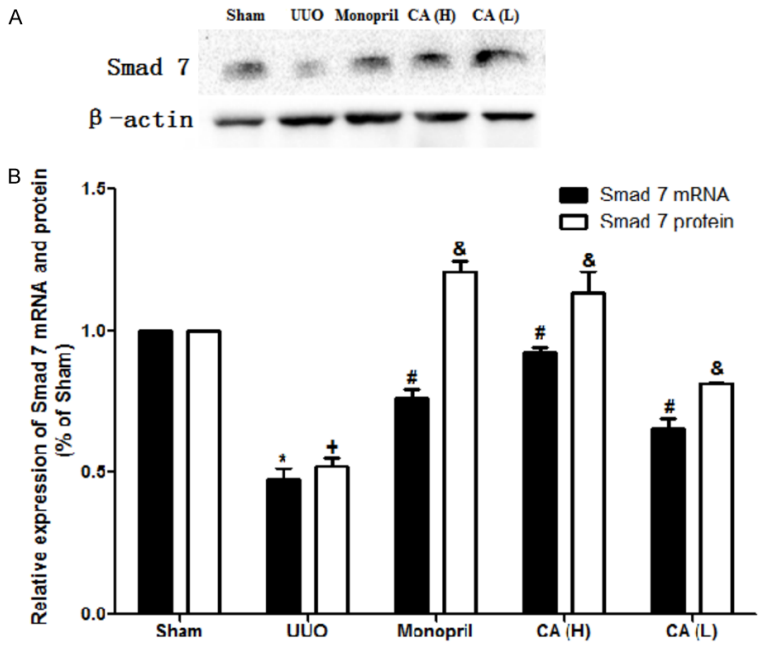

Figure 5. Treatment of CA inhibited Smad7 gene and protein expression in renal tissues of the UUO rats. CA or vehicle control was orally administered in sham- or UUO-operated rats starting on the day of the surgery for 14 days. A. Smad7 was measured by the Western Blot; B. Quantitative data of the Smad7 mRNA and protein expression analyzed for each group. The error bars represent mean ± SD. *P<0.05 compared with Smad7 mRNA level in sham group; #P<0.05 compared with Smad7 mRNA level in UUO group; +P<0.05 compared with Smad7 protein level in sham group; &P<0.05 compared with Smad7 protein level in UUO group.

interstitial damage [16]. Iwano et al. demonstrated that up to 36% of the renal interstitial fibroblasts originated from the local EMT of the kidney tubules. Under normal physiological conditions, the factors that inhibit and promote fibrosis reach a steady state. Meanwhile, renal fibrosis will occur with the onset of homeostatic imbalances.

Smad proteins play a critical role in the TGF-β signal pathway, and also mediate signal transduction. The TGF-β signal is transmitted from the cell membrane to the nucleus, and relies on Smads family proteins regulation. The different intracellular regulatory factors in the Smads signal transduction pathway will have completely different results under the same TGF-β stimulation. For example, transcription will be activated when positive regulatory factors are dominant. Conversely, when the negative regulatory factors are in the dominant position, the transcription will be inhibited. Smad3 is the activated Smad protein, and can promote the formation of kidney fibrosis. The previous research results have proven that it has high expression in the animal model of 5/6 nephrectomy nephropathy, unilateral urethral obstruction (UUO), diabetic nephropathy (DN), and so on. In the rodent model of the DN and UUO, the occurrence and progress of the renal fibrosis has been effectively inhibited through inhibition of Smad3 expression [17]. Smad7 is the inhibitory Smad protein. Many previous research studies have proven that Smad7 can be used as an endogenous TGF-β antagonist to inhibit the TGF-β/Smad signal pathway [6]. Smad7 can also compete with Smad2 or Smad3 to bind with TGF-βR-I or Smad4, and thus is able to inhibit phosphorylation of Smad2/Smad3, and transfer to the cell nucleus. In addition, Smad7 also can induce Smad2 to degrade with the ubiquitin-proteasome of TGF-βR-I, and negatively regulate the TGF-β1/Smad pathway through the ubiquitin ligase-Smad ubiquitination regulatory factors (Smuf1 and Smurf2) [18]. Inhibition of the TGF-β/Smad signal pathway may intervene the normal functioning of an organism. However, the study results have only involved cellular and animal experiments, which still remain at a remote distance from clinical practice.

Modern research studies have found that asiaticoside can inhibit fibroblast proliferation, and inhibit and alleviate the proliferation of fibrous connective tissues, as well as promote the healing of skin wounds. Asiaticoside may provide antioxidant and anti-proliferation effects, as well as immune regulation functions [19, 20]. Pharmacological studies have confirmed that CA may potentially inhibit fibroblast formation, reduce the aggregation of renal interstitial ECM, inhibit the proliferation of mesangial cells, and inhibit glomerular sclerosis [21]. These findings indicate that CA plays an important role in the prevention and treatment of renal fibrosis. However, its mechanism

remains unclear. Previous studies have shown that [22-25] CA may reduce the expressions of the connective tissue growth factor (CTGF) and the monocyte chemoattractant protein-1 (MCP-1) in the kidney tissues of UUO rates. It has also been found to inhibit renal tubular epithelial cells transformed into myofibroblasts and the expression of the bone morphogenetic protein-7 (BMP-7) secreted by the renal tubular epithelial cells cultivated *in vitro*. It can also regulate the balance of matrix metalloproteinase-2/tissue inhibitors of metalloproteinase-2 (MMP-2/TIMP-2) in renal tubular epithelial cells cultivated *in vitro*, further leading to the anti-TIF effect.

Conclusions

In the present study we investigated the treatment effect of CA granula on the UUO rat model. The CA was able to inhibit deposition of lesion kidney collagen fibers and reduce the degree of fibrosis. In addition, the CA could inhibit Smad3 protein expression, and promote Smad7 protein expression, which indicates that CA is able to delay renal tubule interstitial fibrosis after UUO by regulating Smad3 and Smad7 expression. The effects of CA on the fibrosis were found to be dose dependent, and were equivalent to those of fosinopril at the dose of 16.8 mg/100 g/day. This study may potentially provide a theoretical basis for the prevention and treatment of chronic kidney disease with CA granules.

Acknowledgements

This work has been supported by the National Natural Science Foundation of China (No. 81173409).

Disclosure of conflict of interest

None.

Address correspondence to: Dr. Zhu Zhang, Department of Nephrology, The First Affiliated Hospital of Henan Traditional Chinese Medical University, 19 Renmin Road, Zhengzhou 450000, Henan, China. Tel: +86-371-66231932; Fax: +86-371-66220903; E-mail: zhangzhudoc@126.com

References

[1] Yano Y, Fujimoto S, Asahi K and Watanabe T. Prevalence of chronic kidney disease in China. Lancet 2012; 380: 213-4.

[2] Klahr S and Morrissey J. Obstructive nephropathy and renal fibrosis. Am J Physiol Renal Physiol 2002; 283: 861-875.

[3] Kobayashi E, Sasamura H, Mifune M, Shimizuhirota R, Kuroda M, Hayashi M and Saruta T. Hepatocyte growth factor regulates proteoglycan synthesis in interstitial fibroblasts. Kidney Int 2003; 64: 1179-1188.

[4] Eddy AA. Molecular basis of renal fibrosis. Pediatr Nephrol 2000; 15: 290-301.

[5] Razzaque MS and Taguchi T. Cellular and molecular events leading to renal tubulointerstitial fibrosis. Med Mol Morphol 2002; 35: 68-80.

[6] Meng XM, Huang XR, Xiao J, Chung AC, Qin W, Chen HY and Lan HY. Disruption of Smad4 impairs TGF-β/Smad3 and Smad7 transcriptional regulation during renal inflammation and fibrosis in vivo and in vitro. Kidney Int 2012; 81: 266-279.

[7] Inamdar PK, Yeole RD, Ghogare AB and Souza NJD. Determination of biologically active constituents in Centella asiatica. J Chromatogr A 1996; 742: 127-130.

[8] Lee J, Jung E, Kim Y, Park J, Park J, Hong S, Kim J, Hyun C, Kim YS and Park D. Asiaticoside induces human collagen I synthesis through TGFbeta receptor I kinase (TbetaRI kinase)-independent Smad signaling. Planta Med 2006; 72: 324-328.

[9] Bylka W, Znajdek-Awiżeń P, Studzińska-Sroka E, Dańczak-Pazdrowska A and Brzezińska M. Centella asiatica in dermatology: an overview. Phytother Res 2014; 28: 1117-24.

[10] Tang B, Zhu B, Liang Y, Bi L, Hu Z, Chen B, Zhang K and Zhu J. Asiaticoside suppresses collagen expression and TGF-β/Smad signaling through inducing Smad7 and inhibiting TGF-βRI and TGF-βRII in keloid fibroblasts. Arch Dermatol Res 2011; 303: 563-72.

[11] Zeisberg M and Neilson EG. Biomarkers for epithelial-mesenchymal transitions. J Clin Invest 2009; 119: 1429-1437.

[12] Thiery JP, Acloque H, Huang RY and Nieto MA. Epithelial-mesenchymal transitions in development and disease. J Clin Invest 2009; 139: 871-90.

[13] Liu Y. New Insights into Epithelial-Mesenchymal Transition in Kidney Fibrosis. J Am Soc Nephrol 2010; 21: 212-22.

[14] Sabe H. Cancer early dissemination: cancerous epithelial–mesenchymal transdifferentiation and transforming growth factor β signalling. J Biochem 2011; 149: 633-639.

[15] Strutz FM. EMT and proteinuria as progression factors. Kidney Int 2009; 75: 475-481.

[16] Rastaldi MP, Ferrario F, Giardino L, Dell'Antonio G, Grillo C, Grillo P, Strutz F, Müller GA, Colasanti G and D'amico G. Epithelial-mesenchymal

transition of tubular epithelial cells in human renal biopsies. Kidney Int 2002; 62: 137-146.
[17] Lan HY and Chung CK. TGF-β/Smad signaling in kidney disease. Semin Nephrol 2012; 32: 236-243.
[18] Ruan Y, Zhang Z, Zhang X, Liu C and Guo M. The expressions of TGF-beta1 and Smad 2 mRNA on diseased glomeruli and their significance in the development of glomerulosclerosis. Chin J Pathol 2002; 31: 314-7.
[19] Zhang LN, Zheng JJ, Xiao-Hui LI, Meng-Jiao WU, Zhang L and Wan JY. The protective effect of asiaticoside on sepsis-induced acute liver injury in mice. Lishizhen Medicine & Materia Medica Research 2010; 21: 2734-2736.
[20] Dipankar Chandra R, Shital Kumar B and Md Munan S. Current updates on centella asiatica: phytochemistry, pharmacology and traditional uses. Med Plant Res 2013; 3.
[21] Dai LB, Shu P, Yan S, Yue H, Rong L, Ning K, Ye-Yang LI, Xiao-Jian LI, Xie YF and Gang LI. Effects of asiaticoside on dermal fibroblasts in hypertrophic scar. Chin Pharm J 2010; 45: 1067-1072.
[22] Zhang Z, Wang S, Wang B, Zhao L, Wang L and Tang G. Centella asiatica granule on renal tissue in rats with unilateral ureteral obstruction alpha-smooth muscle actin expression. Tradit Chin Med Res 2009; 22: 15-18.
[23] Wang L, Liu P, Ma J, Zhao L, Wang S, Zhang Z, Wang G and Zhang Z. Effect of Centella asiatica granula on TGF-β1-induced expression of bone morphogenetic protein-7 in renal tubular epithelial cells. Shandong Med J 2009; 49: 13-15.
[24] Zhang Z, Wang G, Jiwei MA, Liu H, Zhang X and Zhu G. Effect of herba centellae on the expression of HGF and MCP-1. Exp Ther Med 2013; 6: 427-434.
[25] Zhang Z, Qin Z, Bai J, Liu H, Zhu G and Ma J. Effects of expression of MCP-1, HGF, MMP-2 and TIMP-2 in renal tubular epithelial cell cultured in vitro induced by centella asiatica granule. Chin J Tradit Chin Med Pharm 2015; 2541-2543.